Rare Metal Materials and Engineering
Volume 51, Issue 5, May 2022
Available online at www.rmme.ac.cn

Science Press

Cite this article as: Liu Yao, Zhai Fangyi, Mi Guofa, et al. First-Principles Investigation on Structural, Electronic, Mechanical, and Thermodynamic Properties of Intermetallics in Zr-Be Binary System[J]. Rare Metal Materials and Engineering, 2022, 51(05): 1643-1649.

ARTICLE

First-Principles Investigation on Structural, Electronic, Mechanical, and Thermodynamic Properties of Intermetallics in Zr-Be Binary System

Liu Yao, Zhai Fangyi, Mi Guofa, Liu Chen, Wang Youchao

School of Materials Science and Engineering, Henan Polytechnic University, Jiaozuo 454003, China

Abstract: The first-principles theory calculation was used to investigate the structural, electronic, mechanical, and thermodynamic properties of intermetallics $ZrBe_2$, $ZrBe_5$, $ZrBe_{13}$, and Zr_2Be_{17} in Zr-Be binary alloy system, based on the density functional theory with generalized gradient approximation (GGA) approach. Results show that the optimized lattice parameters at 0 K are in agreement with the available experimental results, indicating the calculation reliability. The calculated formation enthalpy and cohesive energy indicate that all the intermetallics are formed spontaneously at 0 K, among which $ZrBe_5$ has the strongest alloying ability and $ZrBe_2$ has the best structural stability. Subsequently, the electronic density of states (DOS) was also used to investigate the intermetallic stability. The stress-strain method was adopted to calculate the independent elastic constants of the intermetallic. Based on that, the mechanical parameters of polycrystal, such as bulk modulus *B*, shear modulus *G*, Young's modulus *E*, Poisson's ratio *v*, and anisotropy value *A* can be deduced by Voigt-Reuss-Hill approximation. In addition, according to Pugh's criterion, Poisson's ratio, and Cauchy pressure, the ductile behavior of intermetallic was analyzed. As for the thermodynamic properties, all the phonon dispersion curves illustrate the dynamic stability of the intermetallic, and the lattice vibration energy, bulk modulus, thermal expansion coefficient, and specific heat varying with temperature change were calculated by the quasi-harmonic approximation (QHA).

Key words: Zr-Be binary alloy; electronic structure; mechanical properties; thermodynamic properties; first-principles theory

In the past few decades, the intermetallics have attracted considerable interest because of their excellent electronic, magnetic, mechanical, and thermal properties, such as good ductility, thermal stability, high tensile strength, and high corrosion resistance[1-5]. Zirconium (Zr) and Zr-based alloys have excellent physicochemical properties, including the high specific strength, low neutron absorption cross-section, and significant resistance against oxidation, corrosion, and irradiation[6-10]. Therefore, they are widely used in the nuclear industry[11]. Zr-based alloys are also applied in the chemical, marine, medical, and aerospace fields, but their low tensile strength, high melting point, and easy oxidation in smelting process all restrict their application as structural material[12].

The beryllium (Be) has a very low density, low thermal neutron absorption cross-sectional area, high elastic modulus, and high specific strength. Therefore, the Zr-Be binary alloy is a promising material[13]. Based on the Be-Zr binary phase diagram[14], there are four intermetallic compounds: $ZrBe_2$, $ZrBe_5$, $ZrBe_{13}$, and Zr_2Be_{17}. However, the properties of Be-Zr binary intermetallics are rarely reported. Therefore, it is essential to investigate the properties of intermetallics in the Zr-Be binary alloy system.

1 Calculation Method

In this research, the first-principles calculations were performed according to the framework of electronic density functional theory (DFT) through Simulation Package (VASP) with Vienne Ab[15,16]. The generalized gradient approximation (GGA) with Perdew-Burke-Ernzrhof (PBE) method was used to describe the exchange and correlation interactions[17]. The interactions between ions and valence electronics were modelled by the projector-augmented wave (PAW) method[18]. The pseudopotentials of $5s^14d^3$ of Zr and $2s^2$ of Be were

Received date: May 19, 2021
Foundation item: Fundamental Research Funds for University of Henan Province; Natural Science Foundation of Henan Province (182300410266)
Corresponding author: Mi Guofa, Ph. D., Professor, School of Materials Science and Engineering, Henan Polytechnic University, Jiaozuo 454003, P. R. China, Tel: 0086-391-3987478, E-mail: peter@hpu.edu.cn

treated as valance electron configurations. The crystallographic data of the Zr-Be binary intermetallics are listed in Table 1. A plane wave cutoff energy of 400 eV was used. The Brillouin zone integrations were modelled by Monkhorst-Pack[23] k-point mesh, and the k-point mesh was simplified as 9×9×10, 8×8×9, 3×3×3, and 5×5×3 grids for $ZrBe_2$, $ZrBe_5$, $ZrBe_{13}$, and Zr_2Be_{17}, respectively. All structures were fully relaxed. The Zr-Be equilibrium phase diagram[24] exhibits four binary intermetallic compounds: $ZrBe_2$, $ZrBe_5$, $ZrBe_{13}$, and Zr_2Be_{17}. The conventional cell crystalline structures of these intermetallic compounds are shown in Fig.1. Besides, the first-principles calculations of the dynamic matrix and the Fourier transform were conducted by density functional perturbation theory (DFPT)[25-28]. As for DFPT calculations, the supercell of 2×2×2 was used for these Zr-Be intermetallic compounds. The PHONOPY[29] software package was used to acquire the phonon dispersion, phonon density of states, and thermodynamic properties of the intermetallic compounds.

2 Results and Discussion

2.1 Structure

The crystalline structure parameters and optimized lattice parameters of these intermetallic compounds are listed in Table 1. It can be seen that the calculated lattice parameters are close to the experiment values with a deviation of less than 3%, indicating the good accuracy of the calculation, and the deviation between the calculated and experiment values is mainly caused by GGA process and the temperature-dependence of lattice parameters.

2.2 Formation enthalpy and cohesive energy

In order to investigate the thermodynamic stability of the Zr-Be intermetallic compounds, the formation enthalpy and cohesive energy were calculated. In general, the alloying ability of the intermetallic compound can be determined by its formation enthalpy. The formation energy of Zr-Be intermetallic compounds can be evaluated through the composition-averaged energies of the pure elements in their equilibrium crystal structures, as follows:

$$\Delta H = \frac{E_{Zr_xBe_y} - xE^{Zr}_{Solid} - yE^{Be}_{Solid}}{x+y} \quad (1)$$

where ΔH is the formation enthalpy of Zr_xBe_y intermetallics; $E_{Zr_xBe_y}$ is the total energy of Zr_xBe_y intermetallics; E^{Zr}_{Solid} and E^{Be}_{Solid} are the total energies of the most stable ground state structures of Zr and Be, respectively. Therefore, the cohesive energy of Zr_xBe_y intermetallics can be obtained, as follows:

$$E_{coh} = \frac{xE^{Zr}_{Atom} + yE^{Be}_{Atom} - E_{Zr_xBe_y}}{x+y} \quad (2)$$

where E^{Zr}_{Atom} and E^{Be}_{Atom} represent the energy of the isolated Zr and Be atoms, respectively.

The calculated formation enthalpies and cohesive energies of different intermetallic compounds are shown in Fig. 2. All the formation enthalpies are negative, suggesting that the structure of these intermetallic compounds is stable. Furthermore, it can be concluded that $ZrBe_5$ phase has the strongest alloying ability, and the alloying ability of intermetallic compounds is arranged by descending order as follows: $ZrBe_5$>Zr_2Be_{17}>$ZrBe_{13}$>$ZrBe_2$. The calculated cohesive energies of intermetallic compounds are arranged by descending order as follows: $ZrBe_2$>$ZrBe_5$>$ZrBe_{13}$>Zr_2Be_{17}. Thus, $ZrBe_2$ has the largest cohesive energy, indicating that $ZrBe_2$ phase is the most stable phase.

2.3 Electronic properties

The total density of states (TDOS) and partial density of states (PDOS) of different intermetallic compounds were calculated and shown in Fig. 3. All Zr_xBe_y phases exhibit metallic features due to the finite density of states (DOS) values at the Fermi level E_F, and the electronic states near the Fermi level are dominated by Zr 4d states. As for $ZrBe_2$, there is a strong hybridization between Zr 4d and Be 2s states around −4 eV, which is beneficial to structural stability and

Table 1 Calculated and experiment lattice parameters of Zr-Be binary intermetallics

Intermetallic compound	Space group	Wyckoff position	*a*/nm		*b*/nm		*c*/nm		Ref.
			Calculated	Experiment	Calculated	Experiment	Calculated	Experiment	
$ZrBe_2$	P6/mmm (No.191)	Be(2d), Zr(1a)	0.3818	0.3820	0.3818	0.3820	0.3247	0.3240	[19]
$ZrBe_5$	P6/mmm (No.191)	Be(2c), Be(3g), Zr(1a)	0.4570	0.4560	0.4570	0.4560	0.3461	0.3485	[20]
$ZrBe_{13}$	Fm-3c (No.226)	Be(96i), Be(8b), Zr(8a)	0.9997	1.0050	0.9997	1.0050	0.9997	1.0047	[21]
Zr_2Be_{17}	R-3m (No.166)	Be(6c), Be(9d), Be(18h), Be(18f), Zr(6c)	0.7517	0.7540	0.7517	0.7540	1.0981	1.1015	[22]

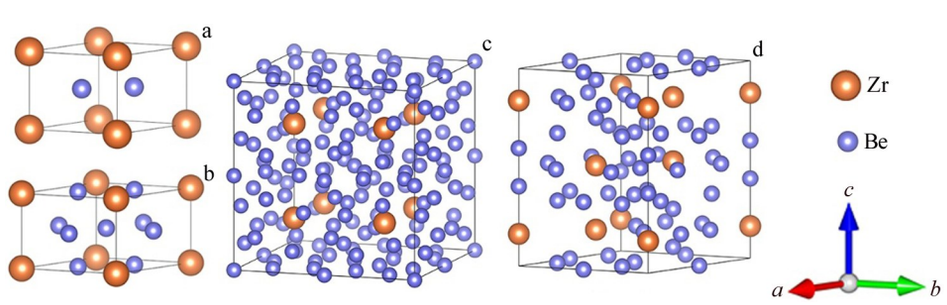

Fig.1 Schematic diagrams of crystalline structures of $ZrBe_2$ (a), $ZrBe_5$ (b), $ZrBe_{13}$ (c), and Zr_2Be_{17} (d) intermetallic compounds

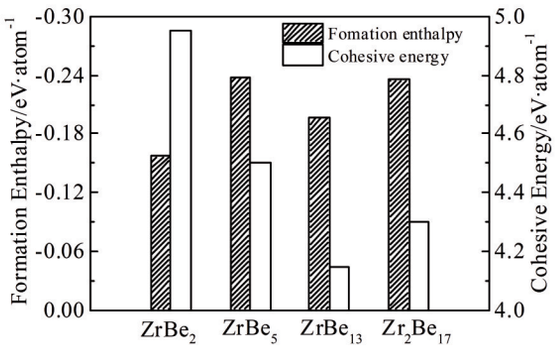

Fig.2 Formation enthalpies and cohesive energies of different Zr-Be intermetallic compounds

mechanical property improvement for the Zr-Be intermetallic compounds.

2.4 Mechanical properties

The stress-strain approach was employed to calculate the elastic properties in this research. Based on Hook's law, a linear relationship exists between stress (σ) and strain (ε). Thus, the proportion of elastic stiffness C_{ij} can be simplified, as follows:

$$\sigma_i = \sum_{j=1}^{6} C_{ij}\varepsilon_j \tag{3}$$

where subscript i and j are positive integer in a specific range. Based on the strain-stress method, the elastic constants can be calculated under pressure of 0 MPa and temperature of 0 K. A small finite strain was applied to the optimized structure, and then the elastic constants were obtained from the stress. The mechanical stability of cubic, hexagonal, and trigonal structures was examined firstly by the Born-Huang mechanical stability criteria, as expressed by Eq. (4~6), respectively:

$$C_{11} > 0, C_{44} > 0, C_{11} - C_{12} > 0, C_{11} + 2C_{12} > 0 \tag{4}$$

$$C_{44} > 0, C_{11} - |C_{12}| > 0, (C_{11} + 2C_{12})C_{33} > 2C_{13}^2 \tag{5}$$

$$\begin{cases} C_{11} > |C_{12}| \\ (C_{11} + C_{12})C_{33} - 2C_{13}^2 > 0 \\ (C_{11} - C_{12})C_{44} - 2C_{14}^2 > 0 \end{cases} \tag{6}$$

The elastic constants of different intermetallic compounds are shown in Table 2, and all the intermetal compounds satisfy the Born-Huang mechanical stability criteria, demonstrating that they are all mechanically stable.

The calculated elastic modulus E and Poisson's ratio v of these intermetallic compounds are listed in Table 3. The resistance to volume change by applied pressure and to shape change against shear stress is measured by the bulk modulus B and shear modulus G, respectively. The larger the value of B and G, the better the resistance to volume change and shape change. It is found that all intermetallic compounds show resistance against the volume change instead of shape change, and there is little difference in the bulk modulus of different intermetallic compounds. In addition, the larger the elastic modulus, the stiffer the materials. Therefore, Zr_2Be_{17} is the stiffest phase among all the Zr-Be binary intermetallic compounds.

The brittle and ductile behavior of materials can be predicted by the ratio of bulk modulus B to shear modulus G[29]. According to the Pugh criterion, the high B/G value corresponds to the ductility; the low B/G value indicates the brittleness. The critical value separating ductility from brittleness is about 1.75. As shown in Table 3, it is concluded that all these intermetallic compounds are brittle, and their ductility is arranged by descending order as follows: $ZrBe_2$>

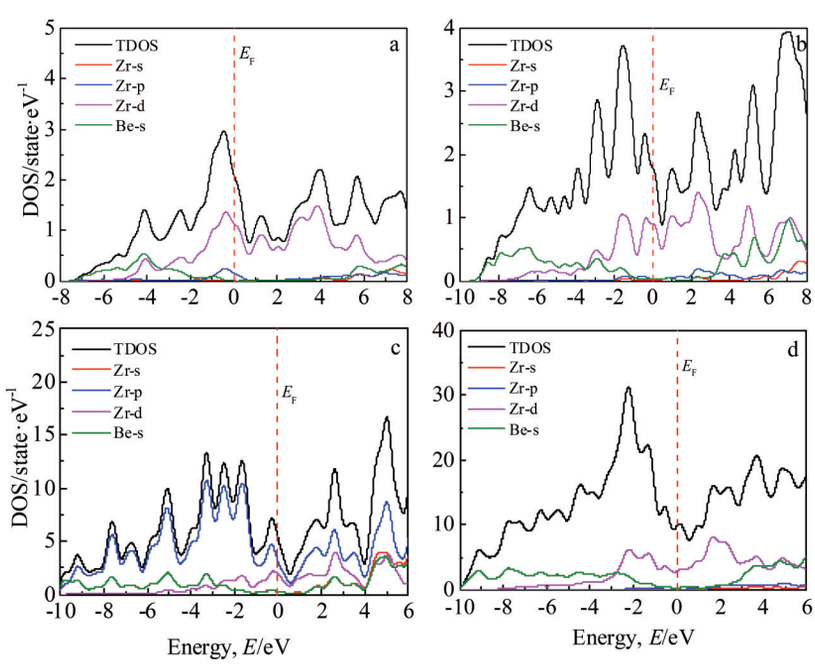

Fig.3 Calculated TDOS and PDOS of different Zr-Be intermetallic compounds: (a) ZrB_2, (b) ZrB_5, (c) ZrB_{13}, and (d) Zr_2B_{17}

Table 2 Calculated independent elastic constants of different Zr-Be intermetallic compounds (GPa)

Intermetallic compound	$ZrBe_2$	$ZrBe_5$	$ZrBe_{13}$	Zr_2Be_{17}
C_{11}	233.26	246.25	319.42	317.82
C_{12}	43.41	90.49	27.79	49.13
C_{13}	87.97	53.33	-	21.98
C_{14}	-	-	-	4.86
C_{33}	196.65	272.56	-	343.16
C_{44}	113.95	158.7	121.3	141.98

Table 3 Calculated mechanical parameters of different Zr-Be intermetallic compounds

Intermetallic compound	$ZrBe_2$	$ZrBe_5$	$ZrBe_{13}$	Zr_2Be_{17}
Bulk modulus, *B*/GPa	122.41	128.80	125.00	129.44
Shear modulus, *G*/GPa	90.56	111.36	130.58	142.33
Elastic modulus, *E*/GPa	217.94	259.34	290.56	312.46
B/*G*	1.35	1.16	0.96	0.91
Poisson's ratio, *v*	0.203	0.164	0.113	0.098

$ZrBe_5$>$ZrBe_{13}$>Zr_2Be_{17}. Besides, Frantsevich et al[30] devised another rule based on Poisson's ratio *v* to predict brittle or ductile behavior of materials, and the critical value is 0.26. The less the value of *v*, the more brittle the materials. Therefore, all these intermetallic compounds show brittleness, which is in good agreement with the results estimated by *B*/*G* criterion.

2.5 Phonon dispersion curves

The phonon frequency is one of the most important aspects for investigation of stability, phase transformation, and thermodynamic properties of the crystalline structures. In order to obtain the phonon dispersion curves with the high-symmetry directions in Brillouin zone, the Hellmann-Feynman theorem and the direct method[31] were employed. The calculated phonon dispersion curves and the corresponding phonon DOS is depicted in Fig.4. The detailed calculation parameters are listed in Table 4.

As shown in Fig.4, there is no imaginary frequency, which indicates the dynamical stability of these intermetallics. The primitive cells of $ZrBe_2$, $ZrBe_5$, $ZrBe_{13}$, and Zr_2Be_{17} intermetallic compounds contain 3, 6, 28, and 19 atoms, and hence, these intermetallics have 9, 18, 84, and 57 independent modes of vibrations, respectively. It is also found that the TDOS is mainly determined by Zr at low frequency, whereas that is dominated by Be at high frequency, because Be atoms are lighter than Zr atoms.

2.6 Thermodynamic properties

The Helmholtz free energies of the intermetallics are calculated by Eq.(7)[32], as follows:

$$F(V,T) = E_0 + F_{el}(V,T) + F_{vib}(V,T) \quad (7)$$

where E_0 is the free energy at 0 K, which can be calculated using VASP directly; F_{el} denotes the electronic contribution to the free energy[33,34]. F_{vib} is the photonic contribution to free energy due to the vibrations of atoms[35-37]. Generally, the entropy contribution due to electrons to the electronic free energy is negligible and E_{el} contribution can be calculated accurately by DFT. Under the quasi-harmonic approximation, F_{vib} can be represented as follows[38-40]:

$$F_{vib}=\frac{1}{2}\sum_{q,v}\hbar\omega_{q,v}(V)+k_BT\sum_{q,v}\ln\left[1-\exp\left(-\hbar\omega_{q,v}(V)/k_BT\right)\right] \quad (8)$$

where q and v are the wave vector and band index, respectively; $\omega_{q,v}$ is the phonon frequency; T, k_B, and $\hbar$ denote the temperature, Boltzmann constant, and the reduced Planck's constant, respectively.

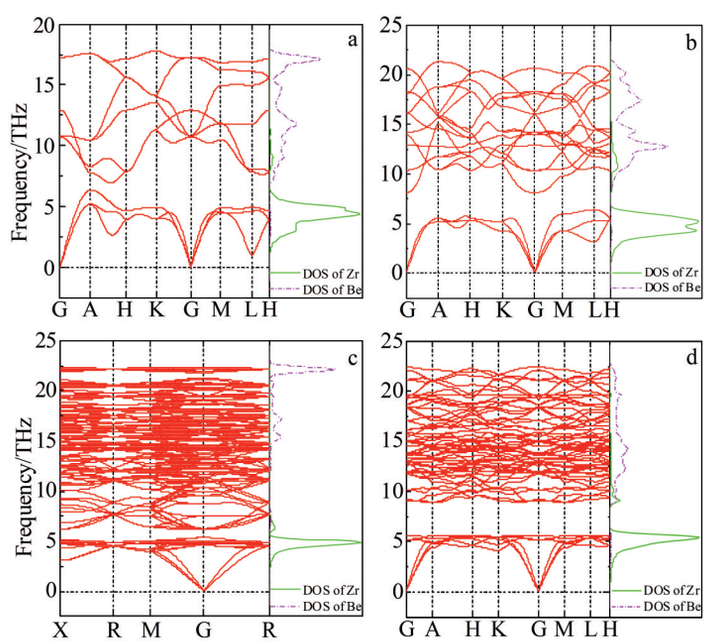

Fig.4 Calculated phonon dispersion curves with DOS of different Zr-Be intermetallic compounds: (a) $ZrBe_2$, (b) $ZrBe_5$, (c) $ZrBe_{13}$, and (d) Zr_2Be_{17}

Table 4 Phonon dispersion calculation parameters of different Zr-Be intermetallic compounds

Intermetallic compund	Brillouin zone path	Number of atoms in a primitive cell	Supercell	k-mesh
$ZrBe_2$	G-A-H-K-G-M-L-H	3	3×3×3	3×3×3
$ZeBe_5$	G-A-H-K-G-M-L-H	6	2×2×2	3×3×3
$ZrBe_{13}$	X-R-M-G-R	28	2×2×2	3×3×3
Zr_2Be_{17}	G-A-H-K-G-M-L-H	38	2×2×2	3×3×3

The vibrational specific heat at constant volume C_V and entropy S can be calculated as a function of temperature, as follows[41,42]:

$$C_V = -T\left(\frac{\partial^2 F_{\text{vib}}}{\partial T^2}\right)_V = \sum_{q,v} k_B \left(\frac{\hbar\omega_{q,v}}{k_B T}\right)^2 \frac{\exp(\hbar\omega_{q,v}/k_B T)}{\left[\exp(\hbar\omega_{q,v}/k_B T) - 1\right]^2} \quad (9)$$

$$S = -\left(\frac{\partial F_{\text{vib}}}{\partial T}\right)_V = \frac{1}{2T}\sum_{q,v}\hbar\omega_{q,v}\coth\left(\frac{\hbar\omega_{q,v}}{2k_B T}\right) - k_B\sum_{q,v}\ln\left[2\sinh\left(\frac{\hbar\omega_{q,v}}{2k_B T}\right)\right] \quad (10)$$

The specific heat at constant pressure C_P can be expressed as follows:

$$C_P = C_V + \alpha^2 BVT \quad (11)$$

where α, B, V, and T represent the linear thermal expansion coefficient, bulk modulus, volume, and temperature of the system, respectively. The linear thermal expansion coefficient α and the volume expansion coefficient α_V can be calculated by Eq.(12), as follows:

$$\alpha = \frac{1}{3}\alpha_V = \frac{1}{3V}\frac{\mathrm{d}V}{\mathrm{d}T} \quad (12)$$

The bulk modulus can be calculated by Eq.(13), as follows:

$$B_T = V\left(\frac{\partial^2 F}{\partial V^2}\right)_T \quad (13)$$

Based on these equations, the Helmholtz free energies of these intermetallic compounds were calculated under the volume value near the equilibrium volume. In Fig. 5, the free energies of the intermetallics as a function of volume at different temperatures are plotted. These curves from the top to the bottom in each figure represent the free energy at temperatures from 0 K to 1000 K with each increment of 100 K. The arc free energy-volume curves are related to the minimum energy and the equilibrium volume. The red lines contain all the minimum energies at different temperatures.

The free energy at 0 K is simply the internal energy of the system, namely the zero-point energy of the system. The free energy of intermetallic compounds is decreased, whereas the internal energy is increased with increasing the temperature. As the internal energy of each intermetallic compound is beyond 200 K, the difference in their free energies is due to different vibrational entropies. The zero-point energy of $ZrBe_2$, $ZrBe_5$, $ZrBe_{13}$, and Zr_2Be_{17} is 3.38 kJ/mol. The $ZrBe_2$ phase is the most stable intermetallic, so its free energy is more negative than others.

The bulk modulus as a function of temperature for all

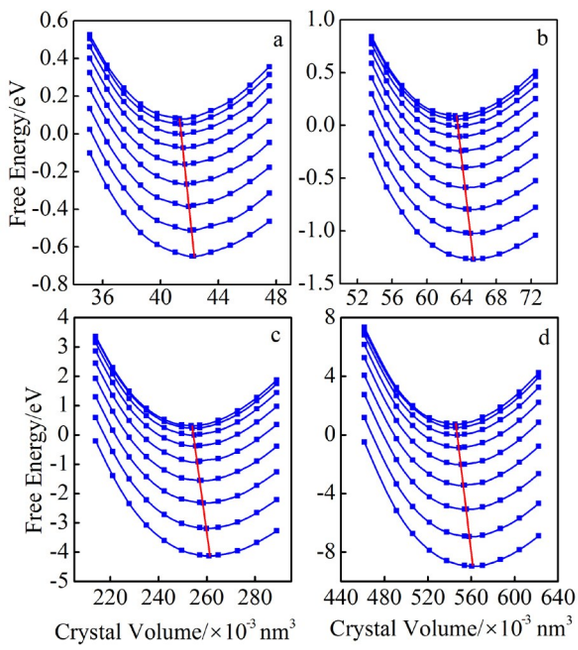

Fig.5 Relationship of free energy-crystal volume at different temperatures of different Zr-Be intermetallic compounds: (a) $ZrBe_2$, (b) $ZrBe_5$, (c) $ZrBe_{13}$, and (d) Zr_2Be_{17}

intermetallic compounds is shown in Fig. 6. The bulk modulus of the intermetallic compounds is decreased with increasing the temperature. The bulk modulus of $ZrBe_2$, $ZrBe_5$, $ZrBe_{13}$, and Zr_2Be_{17} at 0 K is 119.8, 125.8, 122.8, and 126.3 GPa, respectively. The bulk modulus shows small variation in the temperature range of 0~2000 K, which is a favorable feature for the use of waste form. Also, as the bulk modulus of the $ZrBe_2$ phase is less sensitive to the temperature than the other phases ($ZrBe_5$, $ZrBe_{13}$, and Zr_2Be_{17}), the formation of $ZrBe_2$ phase is more desirable.

The linear thermal expansion coefficient α of all intermetallic compounds is shown in Fig. 7. Initially, the linear thermal expansion coefficient of all intermetallic compounds increases sharply. Once the temperature is over 300 K, the thermal expansion coefficient increases slowly, and tends to become a constant value. It can also be found that over 600 K, the thermal expansion coefficient of $ZrBe_2$ is obviously less than that of other intermetallic compounds, which is desirable for the metallic waste form.

The specific heat at constant volume and specific heat capacity at constant pressure of the intermetallic are shown in Fig. 8 and Fig. 9, respectively. It can be seen that at low

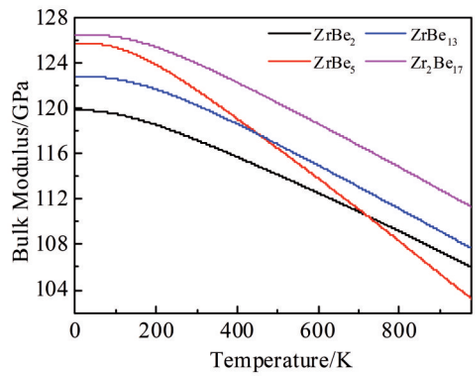

Fig.6 Bulk moduli of different Zr-Be intermetallic compounds

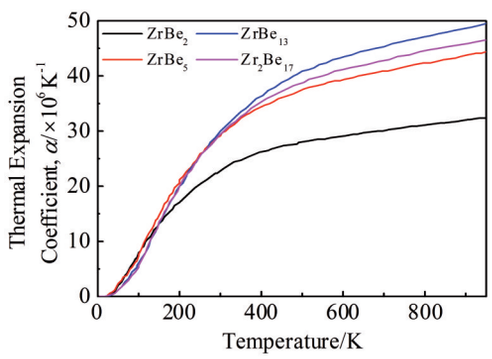

Fig.7 Thermal expansion coefficients α of different Zr-Be intermetallic compounds

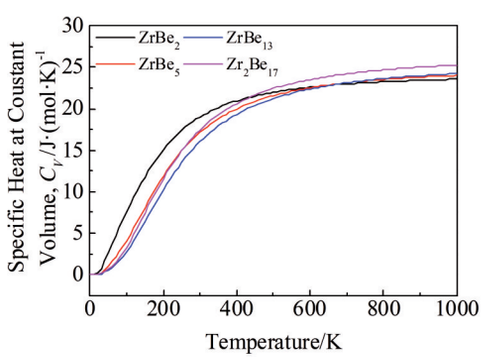

Fig.8 Specific heat at constant volume C_V of different Zr-Be intermetallic compounds

temperature, C_V of all intermetallic compounds increases rapidly at first and once the temperature is over 400 K, C_V becomes almost constant of ~25 J·mol^{-1}·K^{-1}, which is equal to the limit of the specific heat of these intermetallic compounds. Below 400 K, C_V of $ZrBe_2$ is slightly larger than that of $ZrBe_5$, $ZrBe_{13}$, and Zr_2Be_{17}; above 400 K, all these intermetallic compounds show the similar value of C_V. The specific heat at constant pressure C_P of the intermetallic compounds shows the similar behavior to C_V's.

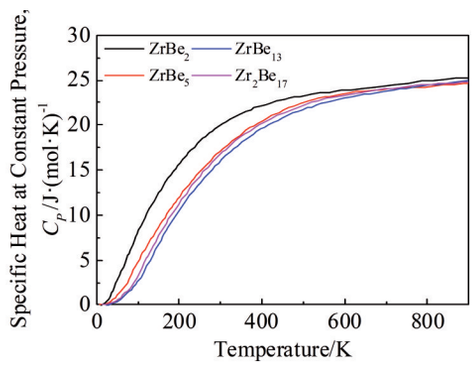

Fig.9 Specific heat at constant pressure C_P of different Zr-Be intermetallic compounds

3 Conclusions

1) All the Zr-Be intermetallic compounds can be formed spontaneously at 0 K, among which $ZrBe_5$ has the strongest alloying ability, and $ZrBe_2$ has the best structural stability.

2) According to different criteria, all the Zr-Be intermetallic compounds show mechanical stability and are brittle at 0 K.

References

1 Diviš M, Kuriplach J. *Physica B: Condensed Matter*[J], 1995, 205(3-4): 353

2 Wu Y, Hu W. *European Physical Journal B*[J], 2007, 60(1): 75

3 Alves T V, Hermoso W, Ornellas F R. *Theoretical Chemistry Accounts*[J], 2010, 127(4): 383

4 Sekkal A, Benzair A, Aourag H *et al. Physica B: Condensed Matter*[J], 2010, 405(13): 2831

5 Pasha S K, Sundareswari M, Rajagopalan M. *Physica B: Condensed Matter*[J], 2004, 348(1-4): 206

6 Xia C Q, Zhang Z G, Feng Z H *et al. Corrosion Science*[J], 2016, 112: 687

7 Chatterjee S, Shah P K, Dubey J S. *Journal of Nuclear Materials* [J], 2008, 383(1-2): 172

8 Cupp C R. *Journal of Nuclear Materials*[J], 1962, 6(3): 241

9 Zhou Y K, Liang S X *et al. Materials Science & Engineering A* [J], 2015, 621: 259

10 Mukherjee P, Nambissan P, Barat P *et al. Journal of Nuclear Materials*[J], 2001, 297(3): 341

11 Garde A. *Standardization News*[J], 1995, 23(2): 28

12 Liang S X, Yin L X, Ma M Z *et al. Materials Science & Engineering A*[J], 2013, 561(3): 13

13 Robert G, Legrand P, Bernard S. *Physical Review B*[J], 2010, 82(10): 104 118

14 Okamoto H. *Journal of Phase Equilibria & Diffusion*[J], 2008, 29(1): 115

15 Hodak M, Wang S C, Lu W C *et al. Physical Review B*[J], 2007, 76(8): 85 108

16 Ma H N, Mi G F, Cheng X Y *et al. Journal of Alloys and Compounds*[J], 2017, 726: 173

17 Perdew J P, Burke K, Ernzerhof M. *Physical Review Letters*[J], 1996, 77(18): 3865
18 Blöchl P E. *Physical Review B*[J], 1994, 50(24): 17 953
19 Zhao Xiaoge, Wang Yong, Zhao Lei *et al*. *Physica Status Solidi B* [J], 2019, 256(10): 1 900 118
20 Zalkin A, Bedford R G, Sands D. *Acta Crystallographica*[J], 1959, 12(9): 700
21 Baenziger N C, Rundle R E. *Acta Crystallographica*[J], 1949, 2(4): 258
22 Collins D M, Delord T J. *Acta Crystallographica*[J], 1984, 40(9): 1497
23 Pack J D, Monkhorst H J. *Physical Review B*[J], 1977, 16(4): 1748
24 Zereg M, Bourki S. *Russian Journal of Physical Chemistry A*[J], 2009, 83(13): 2195
25 Gonze X, Lee C. *Physical Review B*[J], 1997, 55(16): 10 355
26 Audouze C, Jollet F, Torrent M *et al*. *Physical Review B*[J], 2008, 78(3): 35 105
27 Khalil R M A, Hussain M I, Saeed N *et al*. *Optical and Quantum Electronics*[J], 2021, 53(1): 11
28 Togo A, Oba F, Tanaka I. *Physical Review B*[J], 2008, 78(13): 134 106
29 Pugh S F. *Philosophical Magazine*[J], 2009, 45(367): 823
30 Frantsevich I N, Voronov F F, Bokuta S A. *Elastic Constants and Elastic Moduli of Metals and Insulators Handbook*[M]. Kiev: Naukova Dumka, 1983: 60
31 Parlinski K, Li Z Q, Kawazoe Y. *Physical Review Letters*[J], 1997, 78(21): 4063
32 Yu Haili, Dan Xiaohui, Ma Yongjun *et al*. *Chinese Journal of Chemical Physics*[J], 2012, 25(6): 659
33 Arya A, Das G P, Salunke H G *et al*. *Journal of Physics: Condensed Matter*[J], 1994, 18(6): 3389
34 Gayle F W, Sande J B V, McAlister A J. *Bulletin of Alloy Phase Diagrams*[J], 1982, 5(1): 19
35 Caravati S, Bernasconi M, Kühne T D *et al*. *Applied Physics Letters*[J], 2007, 91(17): 171 906
36 Konstantinova T E, Zaitsev V I. *Materials Science and Engineering*[J], 1981, 49(1): 1
37 Kishio K, Brittain J O. *Journal of Physics and Chemistry of Solids*[J], 1979, 40(12): 933
38 Kuriyama K, Saito S, Iwamura K. *Journal of Physics and Chemistry of Solids*[J], 1979, 40(6): 457
39 Uesugi T, Takigawa Y, Higashi K. *Materials Transactions*[J], 2005, 46(6): 1117
40 Chen D, Cang Y P, Luo Y S. *Computational Materials Science* [J], 2015, 106(50): 50
41 Guo X, Podloucky R, Freeman A J. *Physical Review B*[J], 1989, 40(5): 10 912
42 Kresse G, Hafner J. *Physical Review B*[J], 1993, 48(17): 13 115

Zr-Be二元体系金属间化合物结构、电子、力学和热力学性能的第一性原理研究

刘　瑶，翟芳艺，米国发，刘　晨，王友超
(河南理工大学 材料科学与工程学院，河南 焦作 454003)

摘　要：基于密度泛函理论和广义梯度近似（GGA）方法，对Zr-Be二元合金中金属间化合物$ZrBe_2$、$ZrBe_5$、$ZrBe_{13}$和Zr_2Be_{17}的结构、电子、力学和热力学性能进行了第一性原理计算。优化后的0 K点阵参数与已有的实验结果基本一致，证明了计算的可靠性。通过计算得到的形成焓和结合能表明，所有的金属间化合物都能在0 K自发形成，其中$ZrBe_5$的合金化能力最强，$ZrBe_2$的结构稳定性最好。随后，电子态密度（DOS）也被用于了解金属间化合物的稳定性。采用应力-应变法计算了这些金属间化合物的独立弹性常数。在此基础上，利用Voigt-Reuss-Hill近似推导出了多晶材料的体模量B、剪切模量G、杨氏模量E、泊松比v和各向异性A等力学参数。此外，利用Pugh准则、泊松比和柯西压力对金属间化合物的延性行为进行了分析。在热力学性能方面，除了利用准调和近似（QHA）计算晶格振动能量、体模、热膨胀系数和比热随温度变化外，所有的声子色散曲线都说明了这些金属间化合物的动态稳定性。

关键词：Zr-Be二元合金；电子结构；力学性能；热力学性能；第一性原理

作者简介：刘　瑶，女，1996年生，硕士生，河南理工大学材料科学与工程学院，河南 焦作 454003，电话：0391-3987478，E-mail：liuyao0923@outlook.com